Estimation of sediment yield and areas vulnerable to soil erosion and deposition in a Himalayan watershed using GIS

Manoj K. Jain[1,*], Surendra K. Mishra[2] and R. B. Shah[3]

[1]Department of Hydrology, [2]Department of Water Resources Development and Management, Indian Institute of Technology, Roorkee 247 667, India
[3]Department of Irrigation, Government of Nepal, Lalitpur, Kathmandu, Nepal

Erosion is a natural geomorphic process occurring continually over the earth's surface and it largely depends on topography, vegetation, soil and climatic variables and, therefore, exhibits pronounced spatial variability due to catchment heterogeneity and climatic variation. This problem can be circumvented by discretizing the catchment into approximately homogeneous sub-areas using Geographic Information System (GIS). In this study, the remote sensing and GIS techniques (through ERDAS Imagine 8.6 and ArcGIS 9.1 software) were used for derivation of spatial information, catchment discretization, data processing, etc. for the Himalayan Chaukhutia Watershed (India). Various thematic layers for different factors of Universal Soil Loss Equation (USLE) were generated and overlaid to compute spatially distributed gross soil erosion maps for the watershed using 18-year rainfall data. The concept of transport limited accumulation was formulated and used in ArcGIS for generating the transport capacity maps. Using these maps, the gross soil erosion was routed to the catchment outlet using hydrological drainage paths for the derivation of transport capacity limited sediment outflow maps. These maps depict the amount of sediment rate from a particular grid in spatial domain and the pixel value of the outlet grid indicates the sediment yield at the outlet of the watershed. Upon testing, the proposed method simulated the annual sediment yield with less than ±40% error.

Keywords: Geographic Information System, remote sensing, sediment yield, soil erosion, transport capacity, transport limited accumulation.

Introduction

SOIL erosion by water is one of the most important land degradation problems and a critical environmental hazard of modern times worldwide[1]. Accelerated erosion due to human-induced environmental alterations at a global scale is causing extravagant increase of geomorphic process activity and sediment fluxes in many parts of the world[2]. It has been estimated that about 113.3 m ha of land is subjected to soil erosion due to water and about 5334 m tonnes of soil is being detached annually due to various reasons in India[3]. The process of soil erosion involves detachment, transport and subsequent deposition[4]. Sediment is detached from soil surface both by the raindrop impact and the shearing force of flowing water. The detached sediment is transported downslope primarily by flowing water, although there is a small amount of downslope transport by raindrop splash also[5]. Once runoff starts over the surface areas and in the streams, the quantity and size of material transported depends on transport capacity of runoff water. However, if transport capacity is less than the amount of eroded soil material available, then the amount of sediment exceeding the transport capacity gets deposited[4,6]. The amount of sediment load passing the outlet of a catchment is known as the sediment yield. Urbanization, agriculture expansion and deforestation predominantly change the land use due to which soil erosion takes place.

A proper assessment of the erosion problem is greatly dependent on its spatial, economic, environmental and cultural context[7]. The information on sources of sediment yield within a catchment can be used as perspective on the rate of soil erosion occurring within that catchment[8]. Not surprisingly, soil erosion and sediment delivery have become important topics on the agenda of local and national policy makers. This has led to an increasing demand for watershed or regional-scale soil erosion models to delineate target zones in which conservation measures are likely to be the most effective. Despite the development of a range of physically based soil erosion and sediment transport equations, sediment yield predictions at a watershed or regional scale are at present achieved mainly through simple empirical models. Simple methods such as universal soil loss equation (USLE)[9], modified universal soil loss equation (MUSLE)[10] or revised universal soil loss equation (RUSLE)[11], are frequently used for the estimation of surface erosion and then sediment yield in catchment areas[6,12]. They relate the sediment delivery to catchment properties, including drainage area, topography, climate, soil and vegetation characteristics. The main reason why empirical regression equations

*For correspondence. (e-mail: jain.mkj@gmail.com)

are still widely used for soil erosion and sediment yield predictions is their simplicity, which makes them applicable even if only a limited amount of input data is available.

The magnitude of surface erosion and sediment yield is found to vary spatially in a catchment due to the variation in rainfall and catchment heterogeneity. Recent developments in Geographic Information System (GIS) techniques have enhanced the capabilities to handle large databases describing the heterogeneities in land surface characteristics[13]. Remote sensing techniques can be used to obtain spatial information in digital form on landuse and soil type at regular grid intervals with repetitive coverage[14]. Together these tools of remote sensing and GIS have provided the means of identifying the physical factors that control the process of soil erosion and sediment outflow from catchments. The grid or cell approach of catchment sub-division has been used extensively for discretization of catchment into homogenous sub-areas[12,15–17]. The grid or cell approach is quite adaptive to the collection of input data on a regular pattern with the use of remote sensing and GIS, and it accounts for the variation in topographic characteristics over a catchment in detail. Therefore, the objective of this study is to use GIS for descritization of the catchment into small grid-size areas, for computation of such physical characteristics of these areas as slope, land use and soil type which affect the process of soil erosion and deposition in different sub-areas of a catchment. Further, GIS is used for partitioning the catchment grids into overland and channel grids, computation of soil erosion in individual grids, and determination of catchment sediment yield by using the concept of transport limiting sediment delivery.

Methodology

Land use, soil, slope steepness and management parameters are the main factors governing soil erosion potential at a particular location to the erosive power of rainfall. These parameters vary in spatial domain in a catchment. To capture the spatial heterogeneity, a grid-based procedure for discretization of the catchment is adopted in the present study. The USLE is adopted for the estimation of gross erosion rates in the different grids (or cells) of a catchment. The USLE is expressed as

$$SE_i = RKLSCP, \tag{1}$$

where SE_i is the gross amount of soil erosion (MT ha^{-1}); R the rainfall erosivity factor (MJ mm ha^{-1} h^{-1} year^{-1}); K the soil erodibility factor (MT ha h ha^{-1} MJ^{-1} mm^{-1}); LS the slope steepness and length factor (dimensionless); C the cover management factor (dimensionless), and P the supporting practice factor (dimensionless).

Maps for values of the USLE parameters, viz. R, K, LS, C and P factors, can be integrated in ArcGIS using rater calculator to form a composite map denoting gross soil erosion. Estimation of gross soil erosion from grid-sized area of the catchment requires estimates of the various factors appearing in eq. (1). On the basis of correlation between soil erosion and a number of rainfall parameters, the R-factor is defined as the product of total storm energy and maximum 30 min intensity divided by 100 for numerical convenience, known as the EI_{30} index[18,19]. On an annual basis, R-factor is the sum of values of EI_{30} values of the storms in an individual year. Rainfall erosivity estimation using rainfall data with long-time intervals have been attempted by several workers for different regions of the world[20–25]. Using the data for storms from several rain gauge stations located in different zones, linear relationships were established between average annual rainfall and computed EI_{30} values for different zones of India and iso-erodent maps were drawn for annual and seasonal EI_{30} values[26]. The derived relationship is given below

$$R = 79 + 0.363R_N, \tag{2}$$

where R_N is the average annual rainfall in mm. For the present study, eq. (2) is used to compute annual values of R-factor by replacing R_N with actual observed annual rainfall in a year.

For estimation of the LS factor, theoretical relationship based on unit stream power theory[27–29] has been adopted as this relation is best suited for integration with the GIS. The relation is given below

$$LS = \left[\frac{A_s}{22.13}\right]^n \left[\frac{\sin\beta}{0.0896}\right]^m, \tag{3}$$

where A_s is the specific area (= A/b), defined as the upslope contributing area for overland grid (A) per unit width normal to flow direction (b), β the slope gradient in degrees $n = 0.4$ and $m = 1.3$. For channel grid areas, the value of A_s is considered to be equal to the value of the threshold area corresponding to the channel initiation[8].

A grid is considered to lie in the overland region if the size of the area from which it receives the flow contribution is smaller or equal to the specified threshold area for initiation of a channel, while grids receiving flow contribution from area of more than threshold value are considered to form the channel grids[30]. The grids with no flow accumulation lie on the catchment boundary. Different values of channel initiation threshold would result in stream networks with different total stream lengths and consequently with different drainage densities[31]. For the present study, the value of channel initiation threshold is chosen such that total stream length generated using threshold and observed total stream length in 1 : 50,000 scale topographic map (digitized in vector form) are equivalent. The use of eq. (3) in the estimation of the LS-factor allows the introduction of the three-dimensional

hydrological and topographic effect of converging and diverging terrain on soil erosion[32]. The values for the factors *K*, *C* and *P* are computed for different grids on overland and channel region using the information about landuse, soil texture and management practices adopted in catchment[9]. Maps for values of the USLE parameters, viz. *K*, *LS*, *C* and *P* factors were integrated in ArcGIS using rater calculator to form composite map of terms *KLSCP*. The gross erosion estimated using eq. (1) is routed from each cell to the catchment outlet using the concept of transport limiting sediment delivery described below.

Sediment transport and outflow

The eroded sediment from each grid follows a defined drainage path for a particular cell to the catchment outlet as shown in Figure 1. The sediment outflow from a cell is equal to soil erosion in the cell plus the contribution from upstream cells if transport capacity is greater than this sum. However, if transport capacity is less than the sum of soil erosion in the cell and contribution from upstream cells, the amount of sediment exceeding the transport capacity gets deposited in the cell and sediment load equal to transport capacity is discharged to next downstream cell[6]. In the present study, mean annual sediment transport capacity is computed using a relationship based on catchment physical parameters such as soil erodibility, upslope contributing area and slope gradient[33] as given below

$$TC_i = K_{\mathrm{TC}} R K_i A_i^{1.4} S_i^{1.4}, \quad (4)$$

where TC_i is the transport capacity (kg/m^2/yr) of cell i, K_{TC} the transport capacity coefficient and reflects vegetation component within the transport capacity, A_i the upslope contributing area per unit of contour length for cell i and S_i the slope gradient of cell i.

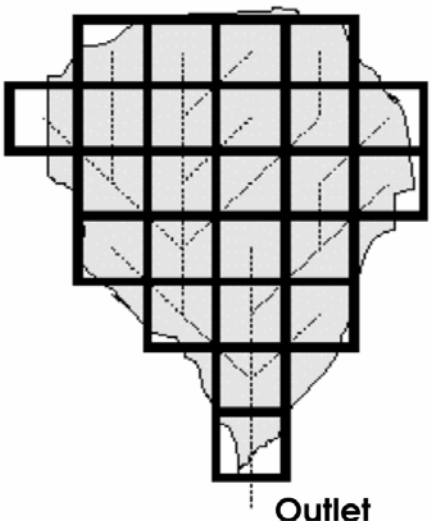

Figure 1. Schematic showing discretized grid cells in a catchment.

Sediment is routed along the runoff paths towards the river taking into account the local transport capacity, TC_i of each pixel. If the local *TC* is smaller than the sediment flux, then sediment deposition occurs. This approach assumes that sediment transport is not necessarily restricted to a transport limited system. If *TC* is higher than the sediment flux, then sediment transport will be supply limited. For the grid-based discretization system adopted herein, transport limited accumulation can be computed as

$$T_{\mathrm{out}_i} = \min(SE_i + \sum T_{\mathrm{in}_i}, TC_i), \quad (5)$$

$$D_i = SE_i + \sum T_{\mathrm{in}_i} - T_{\mathrm{out}_i}, \quad (6)$$

where SE_i is the annual gross soil erosion in cell i, TC_{i} the transport capacity of cell i, T_{in_i} the sediment inflow in cell i from upstream cells, T_{out_i} the sediment outflow from the cell i, and D_i the deposition in cell i.

Use of eqs (1) and (4)–(6) produces different maps of erosion, sediment transport and sediment deposition rates, whereby a distinction is made between gross erosion, net erosion, total sediment deposition and net sediment deposition. Consequently, different total values of erosion and soil loss can be defined. Such maps are of immense use for the identification of critical soil erosion and deposition areas in the catchment.

Study area

The Chaukhutia Watershed located in Almora and Chamoli districts of Uttarakhand, India was selected for the present study (Figure 2). The watershed (29°46′35″–30°06′11″N; 79°11′23″–79°31′21″E) consists of steep hills and valleys interspersed with thick vegetation and drains an area of 572 sq. km (Figure 2). The elevation within this watershed varies between 3099 and 939 m above mean sea level. The slope of general terrain varies from steep to very steep. The watershed under study is dominated by dense mixed forest mainly Pine (*Pinus roxburghii*) and broad-leaved Banj (*Quercus leuchotrichophora*) forest species. Most of the forest areas in the watershed are categorized under reserve forest and cover about 49% of the total area of this watershed. The drainage condition of the catchment is naturally excessively drained. The channel bed in the watershed is rocky or gravelly.

Geological formations in the watershed mainly consist of crystalline and sedimentary rocks of calcareous zone. Crystalline rocks occur as vast sequence of low to medium grade metamorphic associated with coarse to medium grained granites. A thin zone of porphyritic rocks exposed along the Almora fault is known as Chaukhutia Quartz

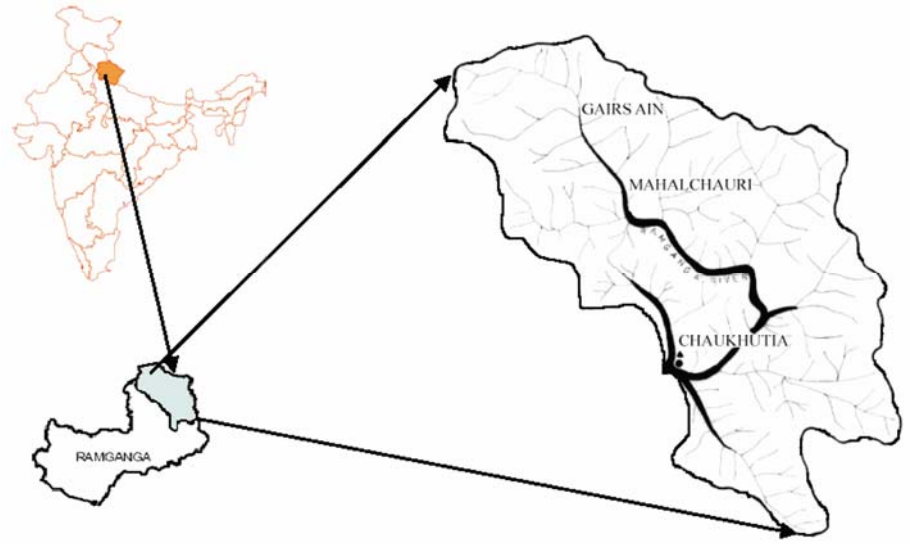

Figure 2. Index map of the study area.

Porphyry. These rocks are highly crushed and fine-grained with porphyro-blasts of quartz and feldspar, and also show development of schistose structure. Sedimentary rocks of Calc zone is found north of Dwarahat around Dhunagiri hill and Ramganga valley near Mehalchauri. Soils in Chaukhutia Watershed vary in texture, depth and slope. The whole catchment of Chaukhutia has been divided into seven soil units[34]. Soils remained more or less fine or course loam skeletal with varied level of gravel. The depth of top soil varies from very shallow to deep soil at different parts of the catchment. The erosion potential of topsoil varies slight to moderate to severe. The soils get saturated even during low intensity rain. Climatologically, the Chaukhutia Watershed lies in sub-Himalayan zone of the Western Himalaya. The variation in altitude influences the climate of the watershed from sub-tropical in the lower region to sub-temperate and temperate in the upper region with a mean annual temperature of 24.5°C.

A significant portion of the total precipitation in the form of rainfall in the watershed occurs mainly during four months of the monsoon, i.e. from June to September with a mean annual precipitation of 1388.7 mm. The monsoon contributes about 74% of the total annual rainfall. The entire hydro-meteorological characteristics of the watershed are characterized by the high precipitation generating peak monsoon flows and low precipitation during the dry season resulting in low flows. The hydro-meteorological data for the watershed are observed by Ramganga Dam Division, Kalagarh (Pauri Garhwal) under the Department of Irrigation, Government of Uttar Pradesh. Stream gauging station for measuring runoff and sediment outflow from Ramganga River at Chaukhutia site. Daily sediment data from January 1973 to December 1990 was collected from irrigation department, site office Kalagarh. The daily sediment yield data was aggregated to annual series and used in the present investigation.

Analysis and discussion of results

Generation of input GIS database

The base map of the study area was prepared using the Survey of India topographic maps at 1 : 50,000 scale. For digital elevation model (DEM), the contours were digitized and interpolated at 50 m pixel resolution using 'topo to raster' command in ArcGIS to create hydrologically correct DEM. The generated DEM was further reconditioned using 'fill sink' command to create depressionless DEM to maintain the continuity of flow to catchment outlet. Location of the outlet of the catchment was marked on DEM and catchment area was delineated using eight direction pour-point algorithm[30]. Figure 3 shows the DEM and delineated catchment boundary. The DEM is then further analysed to distinguish overland and channel grids. The concept of channel initiation threshold is used for defining cells as channel cells.

The landuse map of the study area was prepared by classification of satellite data of Landsat TM which was geo-coded[14] at 30 m pixel resolutions by using the Imagine image processing software[35]. The geo-coded scene was then masked by the catchment boundary derived earlier while delineating the catchment. Landcover map was then generated using the supervised classification scheme with limited ground truthing. Entire area of study catchment is classified into six landcover categories. The attribute values for *C*-factor were assigned to individual grids (Table 1) of Chaukhutia catchment from the tabulated values[9]. The *P*-factor of 0.7 was considered for agricultural lands as many of them follow contour cultivation and unity for other landuse categories.

Soil map of the watershed was digitized from soil survey report prepared by the National Bureau of Soil and Landuse Planning[34]. Details such as fraction of sand, silt,

clay, organic matter and other related parameters information for different mapping units were taken from the same report for Chaukhutia catchment. These soil data were used to derive the soil erodibility (*K*) factor for each mapped soil categories[9]. The values of *K* factor are presented in Table 2.

Use of eq. (1) produces the estimate of gross soil erosion in each of the discretized grids of the catchment. Gross amount of soil erosion for each grid area during a year can be generated by multiplying the term *KLSCP* with the *R*-factor for the corresponding year. The eroded sediment is routed from each grid to the catchment outlet using the concept of transport limiting sediment delivery and deposition described as below.

Generation of the erosion potential map

The erosion potential map of Chaukhutia was developed by overlaying factor maps for *K*, *LS*, *C* and *P*. Numerical value of *KLSCP* term in such maps represents soil erosion potential of different grid cells. Figure 4 shows the areas of varying *KLSCP* values and hence the soil erosion potential in the different cells of the catchment of Chaukhutia. Overlay of Figure 4 on slope and landuse map reveals that a higher cell value coincides with steep slopes and cells with sparse vegetation. High values of this term indicate a higher potential of soil erosion in the cell and vice-versa. The information shown in Figure 4 could be utilized for identification of the sediment source areas of the catchments.

Estimation of gross soil erosion

The magnitude of the gross amount of soil erosion from different descritized cells of the Chaukhutia catchment was computed by integration of the erosion potential map (Figrue 4) with annual values of rainfall erosivity factor *R* (eq. 2). Computed values of annual *R* factor are presented in Table 3 from 1973 to 1990. Gross erosion maps were computed for all years listed in Table 3. Figures 5 and 6 illustrate the gross soil erosion for minimum annual rainfall year 1989 and maximum rainfall year 1978 respectively. Such maps indicate the gross amount of soil erosion

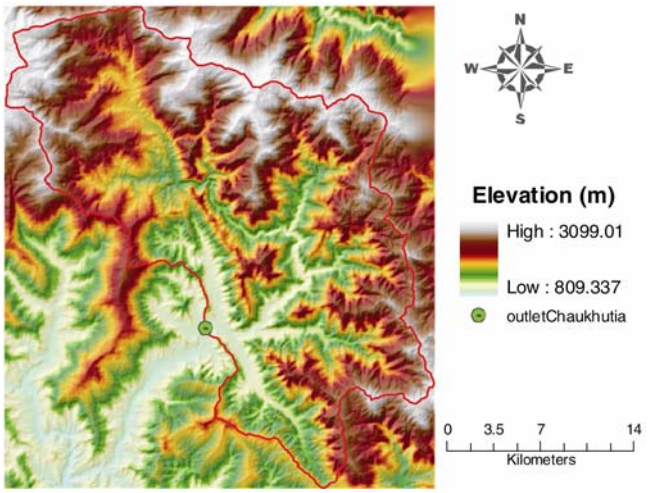

Figure 3. DEM and delineated catchment boundary.

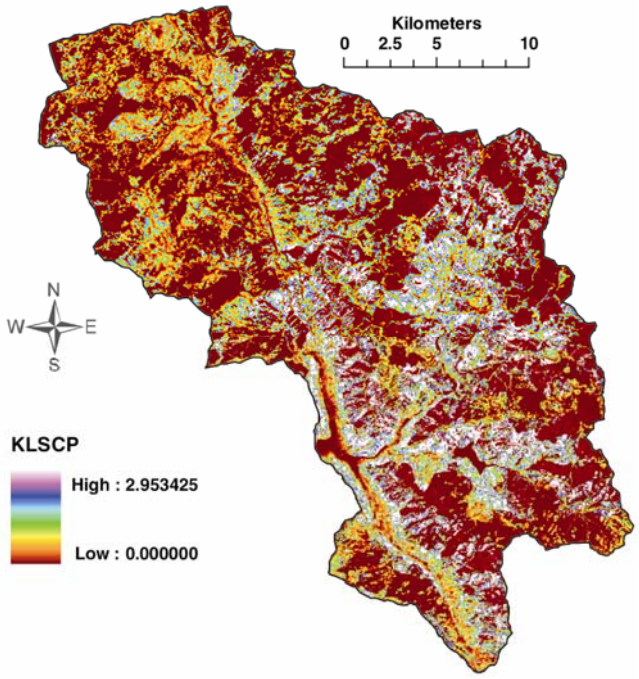

Figure 4. Map depicting variation of *KLSCP* values.

Table 1. Landuse statistics and values of cover management (*C*) factor of Chaukhutia catchment

Landuse	Area (sq. km)	Crop management factor (*C*)
Agriculture	71.2	0.340
Rocky waste land	65.4	0.130
Forest	280.1	0.003
Pasture	91.6	0.200
Water body/river	9.0	0.130
Settlement/roads	54.7	0.130

Table 2. Soil type statistics and values soil erodibility factor (*K*) of Chaukhutia catchment

Type of soil	Area (sq. km)	*K* (t ha h/ ha MJ mm)
Fine loamy to loamy skeletal soils	118.0	0.020
Loamy skeletal to fine loamy soils	103.3	0.023
Coarse loamy soils	57.8	0.032
Sandy skeletal soils	2.4	0.042
Coarse to fine loamy soils	37.3	0.049
Skeletal coarse loamy soils	181.1	0.057
Deep fine loamy to coarse soils	72.1	0.057

Table 3. Computed values of annual *R*-factor for Chaukhutia catchment

Year	*R* ((*MJ* ∗ mm)/(ha ∗ h))	Year	*R* ((*MJ* ∗ mm)/(ha ∗ h))	Year	*R* ((*MJ* ∗ mm)/(ha ∗ h))
1973	681.9	1979	524.8	1985	597.1
1974	NA	1980	609.1	1986	616.7
1975	565.3	1981	461.4	1987	462.4
1976	549.4	1982	602.0	1988	655.0
1977	687.4	1983	641.7	1989	450.2
1978	706.4	1984	484.8	1990	572.7

NA, Data not available.

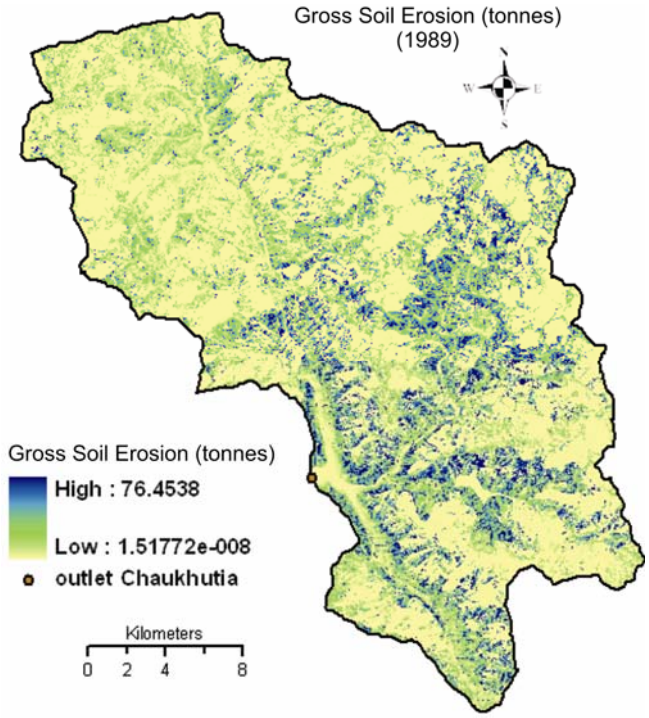

Figure 5. Map depicting gross soil erosion for 1989.

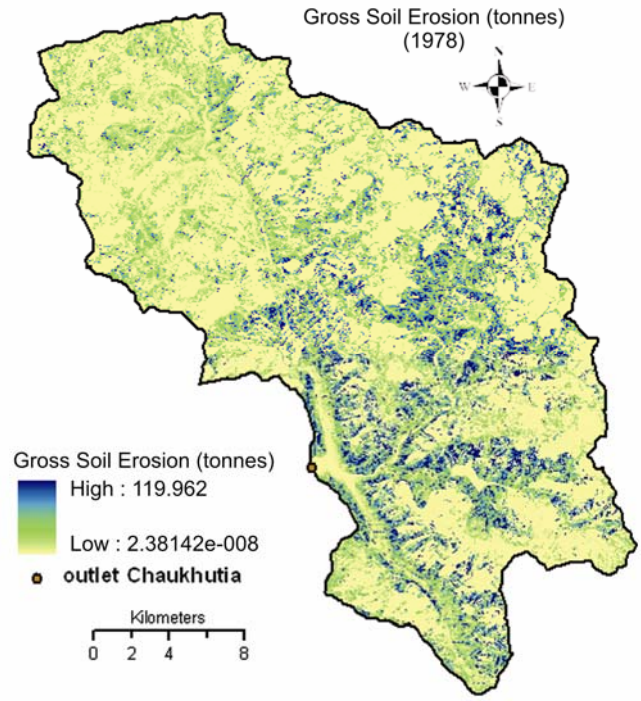

Figure 6. Map depicting gross soil erosion for 1978.

from each cell. It is worth mentioning here that all erosion produced in a cell does not necessarily move from the area and only a part of it finds its way to catchment outlet depending on the transport capacity of the flowing water.

Computation of spatially distributed sediment transport capacity

The amount of eroded soil particles finding its way from upstream to downstream cells and finally to the catchment outlet depends on the transporting capacity of the flowing water. An annual value of spatially distributed transport capacity for all cell areas was computed using eq. (6). Here, mean annual transport capacity varies from year to year as a function of annual rainfall. The parameter transport capacity coefficient (K_{TC}) (eq. 6), which reflects vegetation component within the transport capacity, was determined through calibration[33]. As a first trial, the parameter K_{TC} was taken as unity at the beginning and adjusted manually to minimize sum of the square of the error between the observed and the computed sediment yield determined using the concept of transport limiting accumulation (eq. 10) utilizing observed data for five years. The calibrated value of K_{TC} equal to 0.05 provided a close match between the observed and the computed sediment yield and it was adopted for all other years. This very low value of K_{TC} indicates strong influence of vegetative cover on the reduction of transport capacity of cells. Figure 7 shows transport capacity map for 1975. In the figure, the areas showing higher transport capacity coincide with steep head water areas and channel areas in the catchment, and smaller transport capacity values are mainly found to be associated with the overland regions that surround the confluence of the main stream with the smaller order streams and flatter

land areas found in the cultivated valley lands in the catchment.

Computation of transport limited sediment accumulation and outflow

The gross erosion from each grid was routed downstream (eq. 10) to generate map of the accumulated sediment yield limited by transport capacity. Such maps give

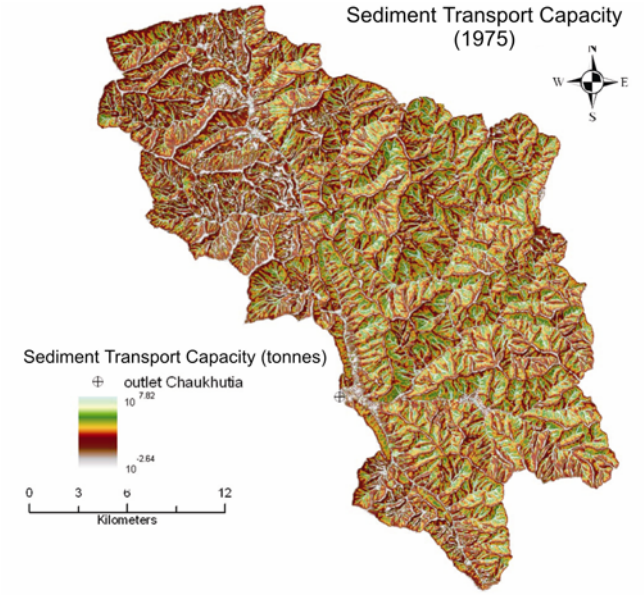

Figure 7. Sediment transport capacity map for 1975.

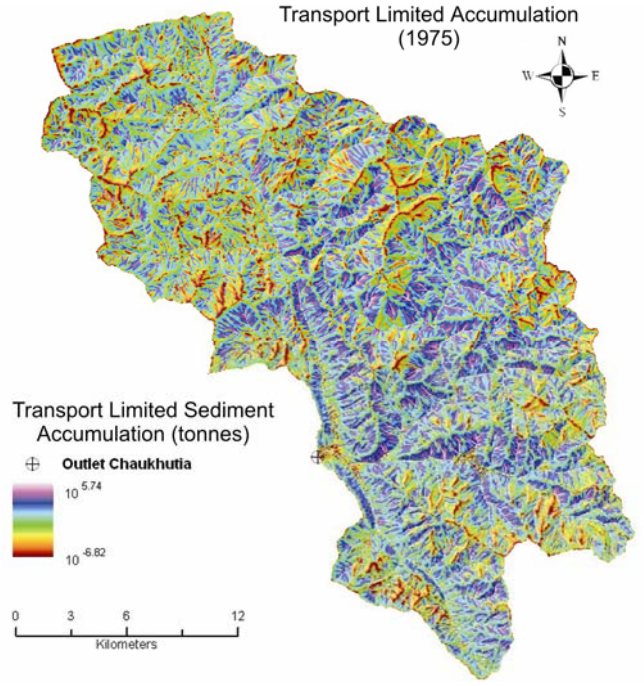

Figure 8. Transport limited sediment outflow map for 1975.

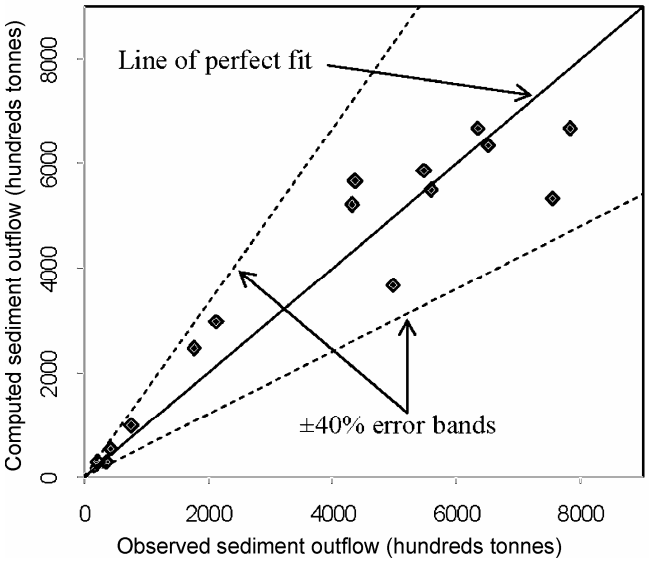

Figure 9. Scatter plot between observed and computed sediment yield.

amount of sediment transported from the system at every grid and are useful for the determination of sediment flowing out of the catchment at any location. Transport limited sediment outflow maps were prepared for all 18 years and Figure 8 depicts map for 1975. The pixel value of the sediment outflow map denotes the amount of sediment leaving the current cell to the next downstream cell. The pixel value of the cell at the catchment outlet denotes the sediment coming out of the watershed. A scatter plot generated based on observed and computed sediment yields revealed that most of the data points were within ±40% error bands (Figure 9). This suggests/indicates that the present method estimates the sediment yield with reasonable accuracy compared to other soil erosion models[12,16,36–38].

Identification of sediment source and sink areas

Maps for deposition of sediment for different years were derived using eq. (6), helpful in the identification of areas vulnerable to silt deposition in the watershed. Also, net erosion maps for different years were calculated by subtracting the deposition rates for each grid cell from the gross erosion rates for each grid cell. Negative values on the net erosion map are the areas where sediment deposition occurs (i.e. true sediment deposition), whereas positive values correspond to grid cells with net sediment erosion. Figure 10 depicts erosion/sediment deposition map for 1975. As seen from this and other such figures (not shown), deposition of sediment resulted at the grids where transport capacity was low, mostly by the sides of some of the stream reaches in valleys and flatter land areas found in the cultivated valley lands in the catchment. It can also be seen from Figure 10 that spatially computed soil removal from most of the catchment

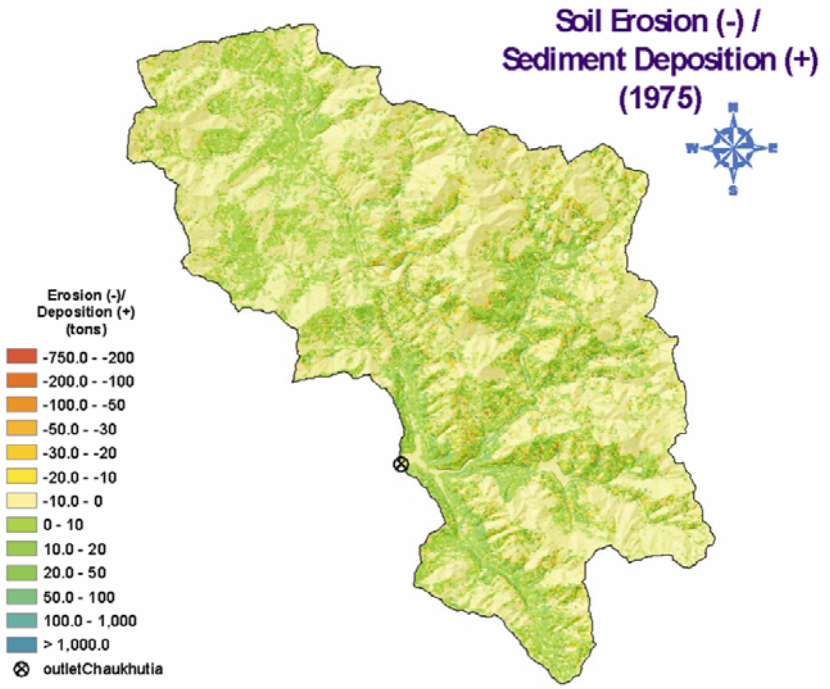

Figure 10. Map depicting soil erosion/sediment deposition areas for 1975.

area is limited to 0–10 tonnes/hectare, except to few pockets which produce more sediment yield. Such maps are extremely important in planning conservation measures; the areas producing more sediment receive priority for their implementation.

Summary and conclusions

Various thematic layers representing different factors of USLE were generated and overlaid to compute spatially distributed gross soil erosion maps for the Chaukhutia Watershed. The concept of transport limited accumulation was used in ArcGIS for generating maps for transport capacity, gross soil erosion was routed to the catchment outlet using hydrological drainage paths resulting in generation of transport capacity limited sediment outflow maps. Such maps provide the amount of sediment flowing from a particular grid in spatial domain. A comparison of the observed and computed sediment yield reveals the proposed method to compute sediment yield with reasonable accuracy. Further, maps for deposition of sediment were also generated for the identification of areas vulnerable to silt deposition in the catchment. The deposition of sediment was found to occur at grids where transport capacity was low, mostly lying by the sides of some of the stream reaches. Superimposition of sediment deposition map over gross erosion map led to areas vulnerable to soil erosion and deposition. Such maps are important in planning conservation and control measures. The specific conclusions are given below:

1. Very low calibrated value of parameter K_{TC} indicates strong influence of vegetative cover on reduction of transport capacity of the cell areas.
2. Areas showing higher transport capacity coincide with steep head water areas and channel areas in the catchment and smaller transport capacity values are mainly associated with the overland regions that surround the confluence of the main stream with the smaller order streams and relatively flat land areas found in the cultivated valley lands in the catchment.
3. The proposed method produces satisfactory estimates of sediment outflow from catchment with $\pm 40\%$ deviation from observations.
4. Spatially computed soil removal from most of the catchment area is limited to 0–10 tonnes/hectare/year except to few pockets which produce more sediment yield.
5. Deposition of sediment resulted at grids where transport capacity was low, mostly lying by the sides of some of the stream reaches in valleys.

1. Eswaran, H., Lal, R. and Reich, P. F., Land degradation: an overview. In *Response to Land Degradation* (eds Bridges, E. M. *et al.*), Science Publishers Inc, USA, 2001, pp. 20–35.
2. Turner, B. L., Clark, W. C., Kates, R. W., Richards, J. F., Mathews, J. T. and Meyer, W. B., *The Earth as Transformed by Human Action*, Cambridge University Press, Cambridge, 1990.
3. Narayan, D. V. V. and Babu, R., Estimation of soil erosion in India. *J. Irrig. Drain Eng.*, 1983, **109**, 419–431.
4. Meyer, L. D. and Wischmeier, W. H., Mathematical simulation of the processes of soil erosion by water. *Trans. Am. Soc. Agric. Eng.*, 1969, **12**, 754–758.

5. Walling, D. E., Erosion and sediment yield research – some recent perspectives. *J. Hydrol.*, 1988, **100**, 113–141.
6. Haan, C. T., Barfield, B. J. and Hayes, J. C., *Design Hydrology and Sedimentology for Small Catchments*, Academic Press, New York, 1994.
7. Warren, A., Land degradation is contextual. *Land Degrad. Dev.*, 2002, **13**, 449–459.
8. Jain, M. K. and Kothyari, U. C., Estimation of soil erosion and sediment yield using GIS. *Hydrol. Sci. J*., 2000, **45**, 771–786.
9. Wischmeier, W. H. and Smith, D. D., Rainfall energy and its relationship to soil loss. *Trans. AGU*, 1958, **39**, 285–291.
10. Williams, J. R., Sediment routing for agricultural watersheds. *Water Resour. Bull.*, 1975, **11**, 965–974.
11. Renard, *et al*., RUSLE, Revised universal soil loss equation. *J. Soil Water Conserv*., 1991, **46**, 30–33.
12. Hadley, R. F. *et al.*, *Recent Developments in Erosion and Sediment Yield Studies*, UNESCO (IHP) Publication, Paris, 1985, p. 127.
13. Jain, M. K., Kothyari, U. C. and Rangaraju, K. G., Geographic Information System based distributed model for soil erosion and rate of sediment outflow from catchments. *J. Hydraulic Eng., ASCE*, 2005, **131**, 755–769.
14. Sabins, F. S., *Remote Sensing: Principles and Interpretations*, W.H. Freeman, New York, 1997, 3rd edn.
15. Beasley, D. B., Huggins, L. F. and Monke, E. J., ANSWERS – a model for watershed planning. *Trans. ASAE*, 1980, **23**, 938–944.
16. Wicks, J. M. and Bathurst, J. C., SHESED: a physically based, distributed erosion and sediment yield component for the SHE hydrological modelling system. *J. Hydrol.*, 1996, **175**, 213–238.
17. Kothyari, U. C., Jain, M. K. and Ranga Raju, K. G., Estimation of temporal variation of sediment yield using GIS. *Hydrol. Sci*., 2002, **47**, 693–705.
18. Wischmeier, W. H. and Smith, D. D., Predicting rainfall erosion losses. Agricultural Handbook no. 537, US Dept of Agriculture, Science and Education Administration, 1978.
19. Wischmeier, W. H., A rainfall erosion index for a universal soil loss equation. *Proc. Soil Sci. Soc. Am.*, 1959, **23**, 246–249.
20. Morgan, R. P. C., *Soil Erosion and Conservation*, Longman Group, Essex, UK, 1995, 2nd edn.
21. Millward, A. and Mersey, J. E., Adapting the RUSLE to model soil erosion in a mountainous tropical watershed. *Catena*, 1999, **38**, 109–129.
22. Mati, B. M., Morgan, R. P. C., Gichuki, F. N., Quinton, J. N., Brewer, T. R. and Liniger, H. P., Assessment of erosion hazard with the USLE and GIS: a case study of the Upper Ewaso Ng'iro North basin of Kenya. *JAG*, 2000, **2**, 78–86.
23. Grimm, M., Jones, R. J. A., Rusco, E. and Montanarella, L., Soil erosion risk in Italy: a revised USLE approach. European Soil Bureau Research Report No 11, EUR 19022 EN, 2003.
24. Natalia, H., Spatial modeling of soil erosion potential in a tropical watershed of the Colombian Andes. *Catena*, 2005, **63**, 85–108.
25. Shamshad, A., Azhari, M. N., Isa, M. H., Wan Hussin, W. M. A. and Parida, B. P., Development of an appropriate procedure for estimation of RUSLE EI_{30} index and preparation of erosivity maps for Pulau Penang in Peninsular Malaysia. *Catena*, 2008, **72**, 423–432.
26. Singh, G., Chandra, S. and Babu, R., Soil loss and prediction research in India, Central Soil and Water Conservation Research Training Institute, Bulletin No T-12/D9, 1981.
27. Moore, I. and Burch, G., Physical basis of the length-slope factor in the universal soil loss equation. *Soil Sci. Soc. Am. J.*, 1986a, **50**, 1294–1298.
28. Moore, I. and Burch, G., Modeling erosion and deposition: topographic effects. *Trans ASAE*, 1986, **29**, 1624–1630; 1640.
29. Moore, I. and Wilson, J. P., Length slope factor for the revised universal soil loss equation: simplified method of solution. *J. Soil Water Conserv*., 1992, **47**, 423–428.
30. Environmental Systems Research Institute (ESRI), Cell based modeling with GRID. Environmental Systems Research Institute Inc., Redlands, California, USA, 1994.
31. Wang, X. and Yin, Z. Y., A comparison of drainage networks derived from digital elevation models at two scales. *J. Hydrol.*, 1998, **210**, 221–241.
32. Panuska, J. C., Moore, I. D. and Kramer, L. A., Terrain analysis: integration into the agricultural nonpoint source (AGNPS) pollution model. *J. Soil Water Conserv*., 1991, **46**, 59–64.
33. Verstraeten, G., Prosser, I. P. and Fogarty, P., Predicting the spatial patterns of hillslope. *J. Hydrol*., 2006, doi:10.1016/j.jhydrol. 2006.10.025.
34. NBSS&LUP, Soils of Uttar Pradesh for optimizing land use: Executive Summary, National Bureau of Soil Survey and Land Use Planning, ICAR, Publication No 68, Nagpur, India, 2004.
35. Earth Resources Data Analysis System (ERDAS), ERDAS Imagine 8.6. ERDAS Inc., Atlanta, Georgia, USA, 2005.
36. American Society of Civil Engineers (ASCE), *Sedimentation Engineering*, American Society of Civil Engineering, New York, NY, 1975.
37. Foster, G. R., Modelling the erosion processes. In *Hydrological Modelling of Small Watersheds* (eds Haan, C. T., Johnson, H. and Brakensiek, D. L.), ASAE Monograph No 5, American Society of Agricultural Engineers, St Joseph, Michigan, 1982, pp. 297–380.
38. Wu, T. H., Hall, J. A. and Bonta, J. V., Evaluation of runoff and erosion models. *J. Irrig. Drain. Eng., ASCE*, 1993, **119**, 364–382.